International Journal of Advanced Science and Research
www.allsciencejournal.com
ISSN: 2455-4227
Received: 07-04-2026, Accepted: 08-05-2026, Published: 23-05-2026
Volume 11, Issue 2, 2026, Page No. 43-55

A deep learning-based approach to estrus detection in swine reproductive management

Ezekiel Olufemi Fasanmi, Abel Efetobor Edje, Umukoro Gift, Chukwuemeka Augustine Obidike
Department of Computer Science, Delta State University Abraka, Delta State, Nigeria

Abstract
Accurate estrus detection and timely insemination are crucial for increasing productivity and economic outcomes in modern large-scale pig farming. Traditional methods of estrus identification, such as the back-pressure test, boar exposure, and physical inspection, are limited by high labor and time intensity, as well as human error. To precisely identify sow estrus. This study presents a deep learning model called YOLOv8n. The model was trained and validated using a dataset gotten from local sources and compared to Random Forest. Experimental data suggest that YOLOv8n obtained an accuracy of 97%, precision of 100%, recall of 95%, f1-score of 97%, and specificity of 100%. This enhanced model consistently distinguishes between estrus and non-estrus, beating the previous model. Validation confirms the model's robust performance in complicated contexts, which approaches expert-level accuracy in estrus identification. YOLOv8 enables consistent, continuous monitoring of estrus status in difficult situations and offers a fresh scientific approach to estrus identification for intensive pig farming.

Keywords: Estrus detection, deep learning, swine reproductive management, YOLOv8n, Sow, Model

Introduction

In today's agricultural landscape, farmers have increasingly embraced animal breeding for diverse objectives such as boosting productivity, fortifying disease resistance, improving reproductive efficiency, and adapting to environmental challenges, notably heat and drought (Almadani *et al*., 2024) [2]. Sow estrus detection and breeding management are critical in swine production. A sow's estrous cycle typically spans 17 to 25 days, averaging 21 days, while estrus itself lasts only about 48.4±1.0 Hours (Duan *et al*., 2025) [7]. Accurately determining the estrus period of sows in modern large-scale pig farming is crucial for optimizing reproductive management. This not only facilitates the precise scheduling of mating, reducing economic losses caused by mistimed or missed inseminations, but also effectively decreases non-productive days, thereby improving litter size and overall reproductive efficiency (Zhao *et al*., 2025) [11]. Our lives nowadays experience sudden, exponential changes in technologies (Akpevwe *et al.*, 2026).

In 2023, China's pig production capacity continued to grow, slaughtering 726.62 million pigs, an increase of 3.81% year-on-year, and pork production reached 57.94 million tons, up 4.6% from 2022 (Cai *et al*., 2025) [4]. The global pork output grew by 0.85% year-on-year, totaling 115.5 million tons. Productivity per sow per year (PSY), defined as the number of weaned piglets per sow annually, is a core indicator of sow reproductive efficiency and the technical level of a pig farm (Cai *et al*., 2025) [4]. Pig Condition Monitoring (PSM) involves multiple disciplines, including signal processing, deep learning and veterinary theory. By analyzing these cross-domain knowledge, the physiological state of pigs can be identified and classified (Chen *et al*., 2021). Current research has indicated that sows may ovulate 10 to 96 h after estrus and that insemination within 0 to 24 h before ovulation can obtain optimal fertility while reducing the number of inseminations (Zheng *et al*., 2023) [12]. Behavioral expression of sow is a reflection of dynamic changes of hormone levels. In estrus, sow rest time decreased, frequency and duration of activity, and standing time increased. Real-time detection of the sow posture helps to automatically monitor their estrus status and health status (Xue *et al*., 2022) [10]. There has been need for individuals and organizations to access computing resources (Obidike *et al*., 2025) [8]

Traditional estrus detection methods rely on manual observation and boar exposure tests, such as the back-pressure test (BPT). However, these methods are labor-intensive and time consuming, making them unsuitable for modern large-scale farms that require automated inspection systems (Duan *et al*., 2025) [7]. Also, these methods have significant limitations, they rely heavily on subjective judgments by technicians, leading to inconsistencies and potential misjudgments. Additionally, they depend on observing sow behaviors, such as standing still or mounting, which can be influenced by environmental and individual differences, which lack objectivity and reliability. Consequently, traditional methods often result in a low estrus detection accuracy, which reduces conception rates (Cai *et al*., 2025) [4]. Vulva swelling and reddening are signs of approaching estrus and are often checked to detect estrus. This occurs due to increased blood flow due to a rise in the estrogen level during estrus events, causing an increase in the vulva size, which can be used as a strong indicator of estrus events (Almadani *et al*., 2024) [2].

The global agricultural landscape is undergoing a profound transformation driven by technological innovations. Among these innovations, machine learning and deep learning have emerged as game-changers, reshaping the way farming operations are conducted (Almadani, Ramos, *et al*., 2024) [3]. With the rapid development of deep learning and artificial intelligence, animal detection methods represented by machine vision have emerged as promising solutions due to their non-contact and cost-effective nature (Zhao *et al*., 2025) [11].

To achieve a highly reliable sow estrus detection system comparable to veterinary experts, this study developed a deep learning-based system to enable accurate estrus detection, providing decision support for artificial insemination.

Materials and Methods

1. Data Collection

The study used a local dataset sourced from Don Henry Farms, Orogun, Ugheli North Local Government Area, and Delta State. The farm has a total of 588 pigs, of which there are 521 female sows and 67 male boars. Pictures of the vulva were taken using high-resolution cameras at varying angles. The vulva images which is the organ for detection of estrus are being captured with a high-resolution camera. These images were instrumental in training and testing the You Only Look Once (YOLO) model for accurate classification and prediction of estrus.

2. Analysis of Developed System

You Only Look Once (YOLO) is a collection of real-time object detection algorithms built on convolutional neural networks. YOLO, which was first proposed by Joseph Redmon *et al.* in 2015, has gone through multiple modifications and enhancements to become one of the most popular object recognition frameworks today. The name "You Only Look Once" refers to the fact that the algorithm makes predictions using only one forward propagation pass through the neural network, as opposed to earlier region proposal-based algorithms such as R-CNN, which require thousands for a single image. Unlike prior methods such as R-CNN and OverFeat, which applied the model to an image at numerous places and scales, YOLO applies a single neural network over the entire image. This network separates the image into regions and calculates bounding boxes and probabilities for each one. These bounding boxes are weighted according to the estimated probabilities.

In this study, a later version of the YOLO model called YOLOv8 will be deployed. YOLO models are popular due to their accuracy and small size. It is a cutting-edge model that can be trained on either powerful or low-end hardware.Alternatively, they can be educated and deployed in the cloud.

Ultralytics, the team behind the revolutionary YOLOv5 model, has launched YOLOv8. It was debuted on January 10, 2023. YOLOv8 detects and classifies items in photos, distinguishing them from one another. Ultralytics improved YOLOv8, making it more user-friendly than YOLOv5. This improved model builds on the success of YOLOv5 by improving its power and user-friendliness in computer vision tasks. The enhancements include a changed backbone network, anchor-free detecting head, and a revised loss function. Furthermore, it includes built-in capability for image classification. YOLOv8 is distinctive in that it delivers unmatched speed and accuracy performance while maintaining a streamlined design that makes it suitable for different applications and easy to adapt to various hardware platforms (Sohan *et al.*, 2024).

Architecture of the developed model

The YOLOv8 architecture consists of two key components: the backbone and the head, both of which employ a fully convolutional neural network.

Backbone: YOLOv8 has a new backbone network that is a modified version of the CSPDarknet53 design. This architecture comprises of 53 convolutional layers and uses a technique known as cross-stage partial connections to improve information transfer throughout the network's various tiers. YOLOv8 uses sequential convolutional layers to extract meaningful characteristics from input images. The new C2f module combines high-level features with contextual information to improve detection accuracy. The SPPF module and subsequent convolution layers process features at varying sizes.

The head examines the Backbone's feature maps to generate bounding boxes and object classes for the model. YOLOv8's detachable head maintains objectness scores, classification, and regression independently. This technique improves model accuracy by allowing each branch to focus on its specific task. Figure 1 shows the U layers (also known as upsample layers). Increase the resolution of the feature maps. The head employs convolutional layers to analyze feature maps, followed by a linear layer that predicts bounding boxes and class probabilities. The head's architecture prioritizes speed and accuracy, with a focus on channel count and kernel size for optimal performance.

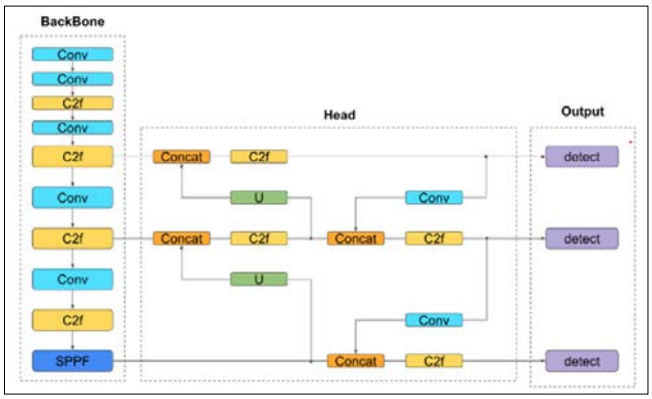

Fig 1: YOLOv8 Architecture visualization (Sohan et al., 2024)

The Detection module applies convolution and linear layers to convert high-dimensional information into bounding boxes and object classifications. The structure is designed for speedy and accurate item detection.

YOLOv8, like YOLOv6 and YOLOv7, is an anchor-free model. This method predicts an object's center directly, rather than using a known anchor box as an offset. Early YOLO models (YOLOv5 and earlier) faced challenges with anchor boxes, which could only represent the target benchmark's box distribution and not the custom dataset's distribution. Anchor-free detection reduces the amount of box predictions, accelerating Non-Maximum Suppression (NMS), a post-processing phase that evaluates potential detections after inference.

The YOLO architecture's convolutional (conv) layers use learnable filters to recognize features in input images. These layers detect features at various scales and resolutions, enabling the network to identify objects of diverse forms and sizes. The output of these layers is sent via other layers to provide bounding boxes and class predictions for detected objects in the image. Unlike YOLOv5, YOLOv8 employs a separate convolution layer known as C2f. This new layer replaces the C3 layer from YOLOv5. In YOLOv8, the C2f layer concatenates the outputs of all Bottleneck layers, while YOLOv5's C3 layer just uses the output of the last Bottleneck layer. Figure 2 shows the C3 module of YOLOv5

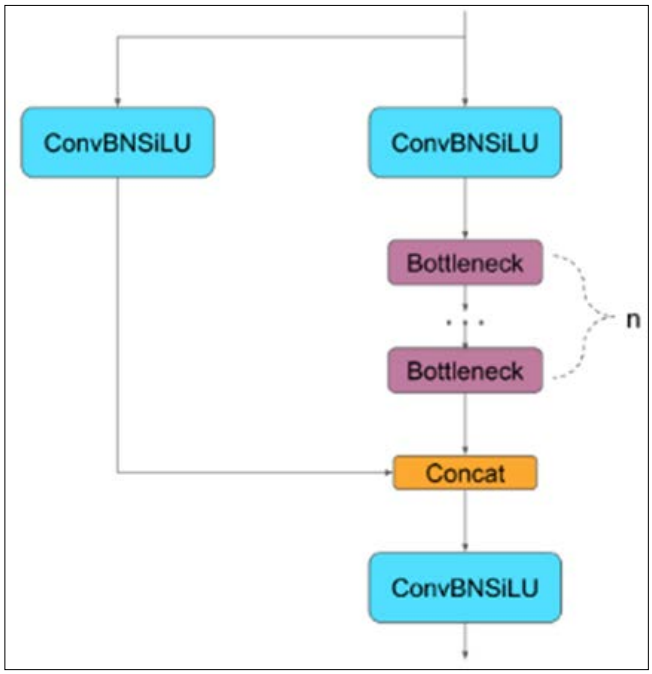

Fig 2: C3 Module of YOLOv5, the number of bottleneck layers are n. ConvBNSiLU is a block composed of a Conv, a BatchNorm and a SiLU layer (Sohan et al., 2024)

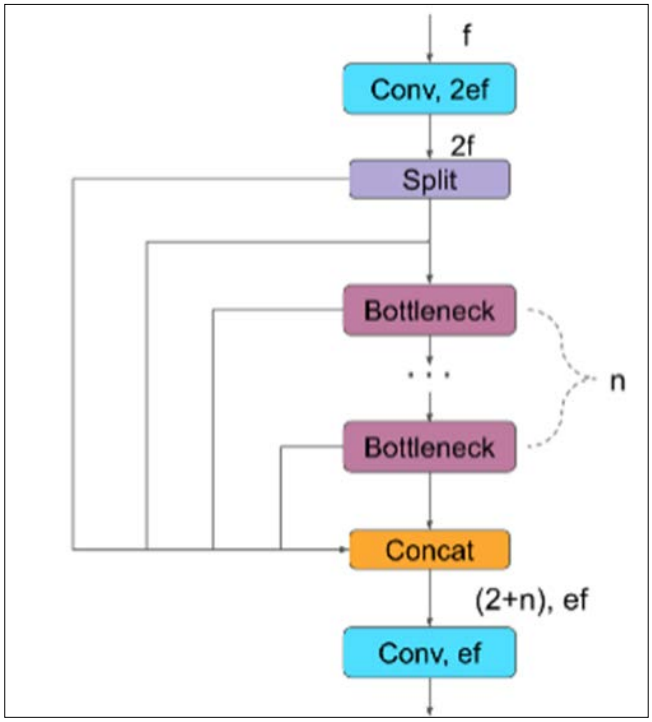

Fig 3: C2f Module of YOLOv8, Conv is a block composed of a Conv2d, a BatchNorm and a SiLU layer (Sohan et al., 2024)

This system's bottleneck is similar to that of YOLOv5, but with a modified initial convolution layer. The kernel size has been raised from 1x1 to 3x3, matching the ResNet block specified in 2015. The system's neck concatenates features without requiring the same channel dimensions, resulting in fewer parameters and smaller tensors overall.

Advantages of the developed model

1. YOLOv8 employs cutting-edge backbone and neck designs, resulting in better feature extraction and object detection performance.
2. YOLOv8 uses an anchor-free split Ultralytics head, which adds to greater accuracy and efficiency in detection when compared to anchor-based techniques.
3. YOLOv8 is ideal for real-time object detection jobs in a variety of application fields since it prioritizes maintaining an optimal mix of accuracy and speed.
4. YOLOv8 provides a variety of pretrained models to address diverse jobs and performance needs, making it easier to pick the best model for your individual use case.

Performance Metrics

The trained model is rigorously assessed using metrics critical to clinical diagnostics, including precision, f1-score, accuracy, specificity, Recall and the area under the curve (AUC)..AUC provides an overall measure of the model's classification capability.

Cross-validation is employed to ensure the model generalizes well across different data subsets. Performance across folds is averaged to evaluate consistency. Additionally, comparisons traditional support vector machine help establish the proposed model's superiority in terms of accuracy, efficiency, and scalability.

Table 1: Confusion Matrix

	Predicted Positive (Disease)	**Predicted Negative (Healthy)**
Actual Positive (Disease)	True Positive (TP): Correctly identified estrus	False Negative (FN): estrus incorrectly classified
Actual Negative (Healthy)	False Positive (FP): non-Estrus incorrectly classified as estrus	True Negative (TN): Correctly identified non-estrus

Recall: Is a metric that expresses how frequently it properly selects positive examples, or true positives, out of all the real positive samples in the dataset. Recall can be computed by dividing the total number of positive cases by the number of true positives, as depicted in equation 3.15

$$Recall = \frac{TP}{TP+FN} \quad (1)$$

FI-Measure: The weighted harmonic mean of the system's recall and precision is known as the F- measure. It is a metric for assessing a model's precision on a dataset. It is employed in the assessment of binary classification schemes that categorize instances as either "positive" or "negative', as denoted in equation 3.16.
(2)

$$F1 - score = \frac{2 \times Recall \times Precision}{Recall + Precision} \quad (2)$$

Precision: Is the ratio of true positive predictions to total positive predictions and is computed using equation 3.17
(3)

$$p = \frac{TP}{TP+FP} \quad (3)$$

Accuracy measures the overall correctness of a model:
(4)

$$A = \frac{TP+TN}{TP+TN+FP+FN} \quad (4)$$

Specificity: it measures the proportion of actual negative cases that a model correctly identifies as negative.
(5)

$$S = \frac{TN}{TN+FP} \quad (5)$$

Experimental setup

In the developed Estrus detection System, estrus and non-estrus images were classified using a deep learning model based on YOLOv8 model. The system was developed and implemented using Python programming language. Ultralytics, numpy, sklearn, and TensorFlow, OpenCV, and Keras libraries are also used. The YOLOv8 model was trained on a curated dataset consisting of 490 vulva images. These images were obtained from a local farm in Delta state. Each image was preprocessed by resizing to 224×224 pixels, normalized to a [0, 1] scale, and divided into training, testing, and evaluation sets using a 70:15:15 ratio. In the training configuration, 70% of the data was used for model training, while 15% were used for testing and the remaining 15% for evaluation. A learning rate of 0.001 and batch size of 16 were used during model training for 50 epochs. The model employed typical CNN layers including convolution, pooling, flatten, and dense layers, followed by a softmax output layer for classification. The model's performance was further evaluated using confusion matrix analysis, achieving high precision, recall, and F1-score across all classes. The robustness of the system is evident in its consistent classification accuracy and fast inference time, making it suitable for real-time detection.

Results and Discussion

This section presents the outcomes of the trained YOLOv8 model designed for predicting retinal diseases. The performance of the system is evaluated using various metrics, including accuracy, precision, specificity, recall, F1-score, and confusion matrices, to assess the model's effectiveness in diagnosing different types of retinal conditions from medical images. The results are discussed in detail, comparing the model's performance against existing approaches and highlighting any notable trends or patterns observed during the testing phase. Additionally, the strengths and limitations of the developed system are examined, providing insights into areas where improvements can be made for better diagnostic accuracy and clinical applicability.

1. Training results: Accuracy and loss metrics

Here's the table for the 50 epochs, showing time, training accuracy, training loss, validation accuracy, and validation loss: Loss: Measures how far the model's predictions are from the actual labels. It's a continuous value (e.g., 0.4, 1.2, etc.) based on a loss function like categorical_crossentropy. Accuracy: Measures how many predictions the model got right (e.g., 70%, 90%). It's a percentage of correct predictions.

Table 2: Accuracy and loss metrics

Epoch	Time	Train/loss	Metrics/accuracy_top1	Metrics/accuracy_top5	Val/loss	Lr/pg0	Lr/pg1	Lr/pg2
1	26.6039	0.70123	0.91304	1	0.51381	0.000167	0.000167	0.000167
2	47.4076	0.30702	0.95652	1	0.10929	0.000343	0.000343	0.000343
3	66.9041	0.07647	1	1	0.00753	0.000512	0.000512	0.000512
4	85.4724	0.01564	1	1	0.00086	0.000674	0.000674	0.000674
5	103.774	0.00593	1	1	0.00095	0.000829	0.000829	0.000829
6	122.793	0.00761	1	1	0.00021	0.000976	0.000976	0.000976
7	140.92	0.00332	1	1	0.0001	0.001116	0.001116	0.001116
8	159.19	0.00238	1	1	0.00015	0.001249	0.001249	0.001249
9	177.673	0.00067	1	1	7.00E-05	0.001375	0.001375	0.001375
10	196.074	0.00614	1	1	6.00E-05	0.00137	0.00137	0.00137
11	214.424	0.0017	1	1	7.00E-05	0.001337	0.001337	0.001337
12	233.636	0.00511	1	1	6.00E-05	0.001304	0.001304	0.001304
13	254.224	0.03123	1	1	8.00E-05	0.001271	0.001271	0.001271
14	272.179	0.03795	1	1	0.00035	0.001238	0.001238	0.001238
15	289.996	0.01503	1	1	0.00075	0.001205	0.001205	0.001205
16	307.829	0.01778	1	1	0.00097	0.001172	0.001172	0.001172
17	325.51	0.02504	1	1	0.00283	0.001139	0.001139	0.001139
18	344.743	0.01235	1	1	0.0011	0.001106	0.001106	0.001106
19	363.708	0.00391	1	1	0.00097	0.001073	0.001073	0.001073
20	381.982	0.00554	1	1	0.00018	0.00104	0.00104	0.00104
21	399.965	0.00308	1	1	0.00011	0.001007	0.001007	0.001007
22	418.033	0.00188	1	1	7.00E-05	0.000974	0.000974	0.000974
23	436.137	0.00255	1	1	3.00E-05	0.000941	0.000941	0.000941
24	454.274	0.00072	1	1	7.00E-05	0.000908	0.000908	0.000908
25	472.447	0.00086	1	1	2.00E-05	0.000875	0.000875	0.000875
26	490.663	0.00068	1	1	3.00E-05	0.000842	0.000842	0.000842
27	508.659	0.02969	1	1	3.00E-05	0.000809	0.000809	0.000809

28	526.988	0.00792	1	1	0.00165	0.000776	0.000776	0.000776
29	545.935	0.00525	1	1	0.00097	0.000743	0.000743	0.000743
30	564.204	0.00209	0.98551	1	0.00902	0.00071	0.00071	0.00071
31	582.373	0.00246	0.98551	1	0.16572	0.000677	0.000677	0.000677
32	600.436	0.00158	0.98551	1	0.01055	0.000644	0.000644	0.000644
33	618.453	0.01486	0.98551	1	0.00685	0.000611	0.000611	0.000611
34	636.835	0.00289	1	1	0.0001	0.000578	0.000578	0.000578
35	655.187	0.00219	1	1	4.00E-05	0.000545	0.000545	0.000545
36	673.256	0.00098	1	1	5.00E-05	0.000512	0.000512	0.000512
37	691.367	0.00112	1	1	2.00E-05	0.000479	0.000479	0.000479
38	709.381	0.00054	1	1	2.00E-05	0.000446	0.000446	0.000446
39	727.457	0.00201	1	1	2.00E-05	0.000413	0.000413	0.000413
40	745.708	0.00313	1	1	2.00E-05	0.00038	0.00038	0.00038
41	764.046	0.0006	1	1	5.00E-05	0.000347	0.000347	0.000347
42	782.171	0.00058	1	1	2.00E-05	0.000314	0.000314	0.000314
43	800.35	0.00048	1	1	2.00E-05	0.000281	0.000281	0.000281
44	818.464	0.00041	1	1	1.00E-05	0.000248	0.000248	0.000248
45	837.073	0.00026	1	1	1.00E-05	0.000215	0.000215	0.000215
46	855.472	0.00148	1	1	1.00E-05	0.000182	0.000182	0.000182
47	873.497	0.00064	1	1	2.00E-05	0.000149	0.000149	0.000149
48	891.617	0.00064	1	1	1.00E-05	0.000116	0.000116	0.000116
49	909.763	0.01013	1	1	1.00E-05	8.27E-05	8.27E-05	8.27E-05
50	927.879	0.00496	1	1	4.00E-05	4.97E-05	4.97E-05	4.97E-05

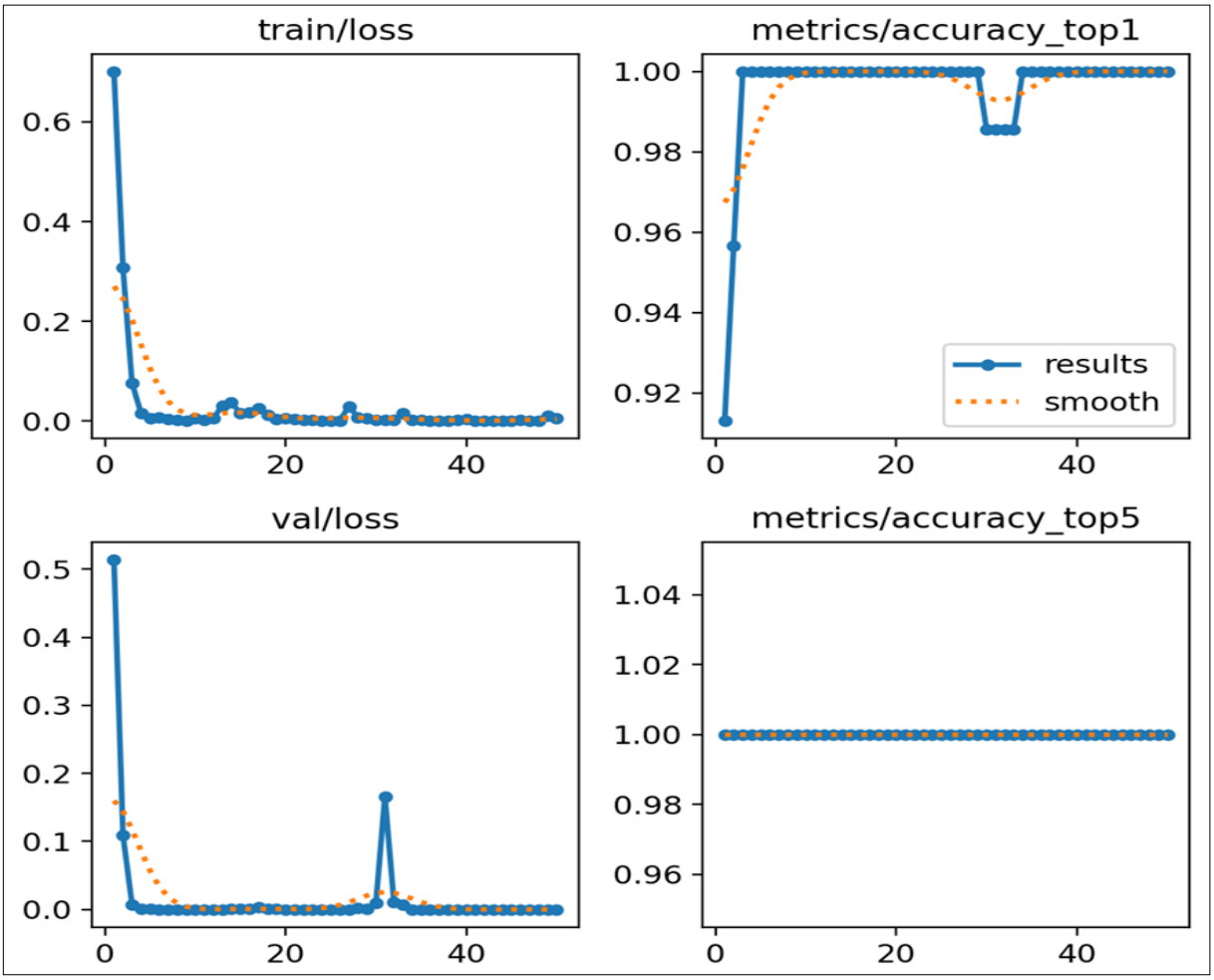

Fig 4: Train and loss results

Batch results

This section shows results gotten from model during training as the data were arranged in batches for training.

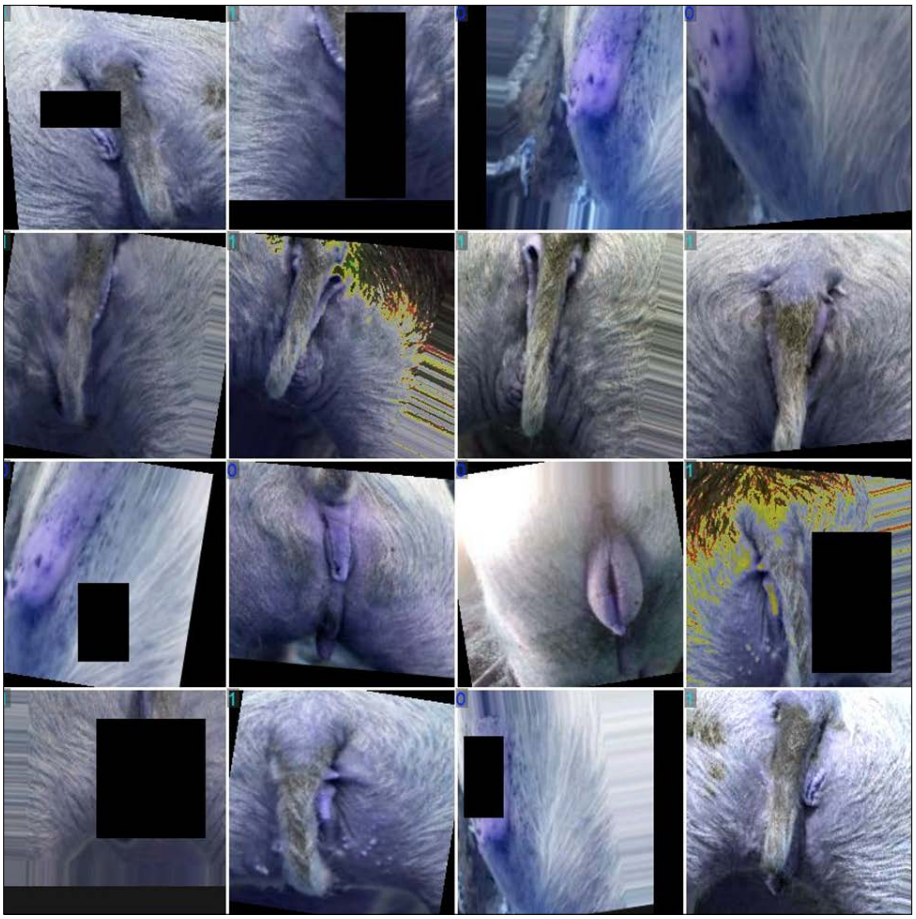

Fig 5: train batch0

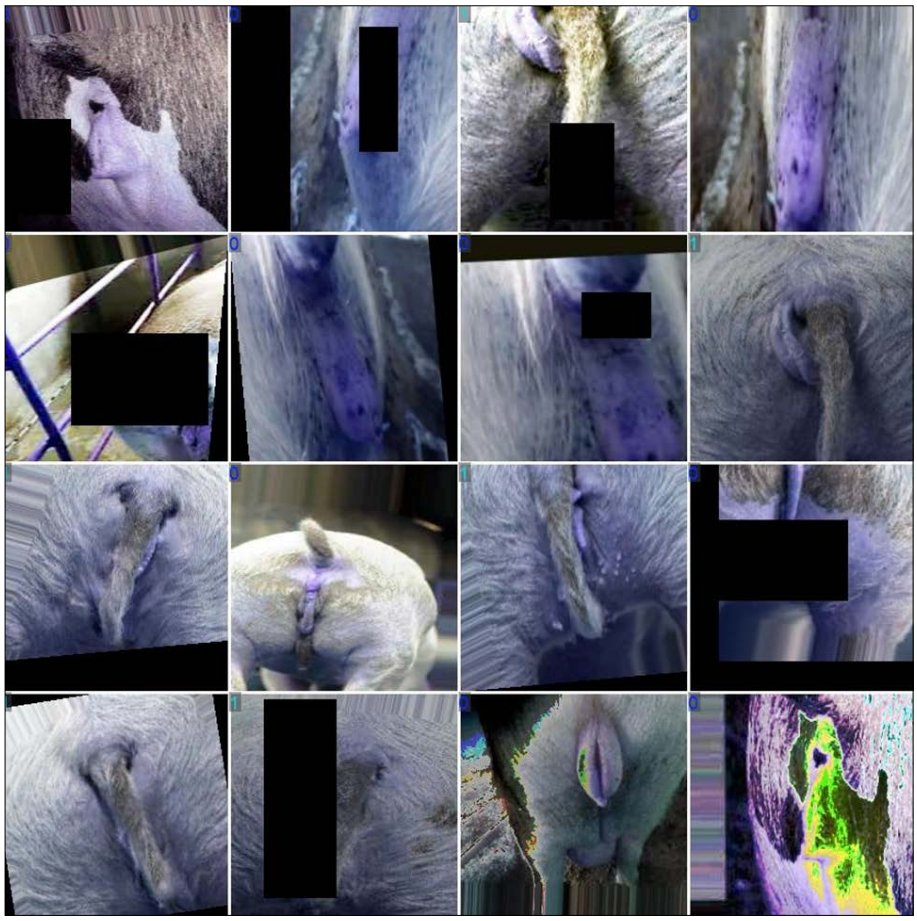

Fig 6: train batch1

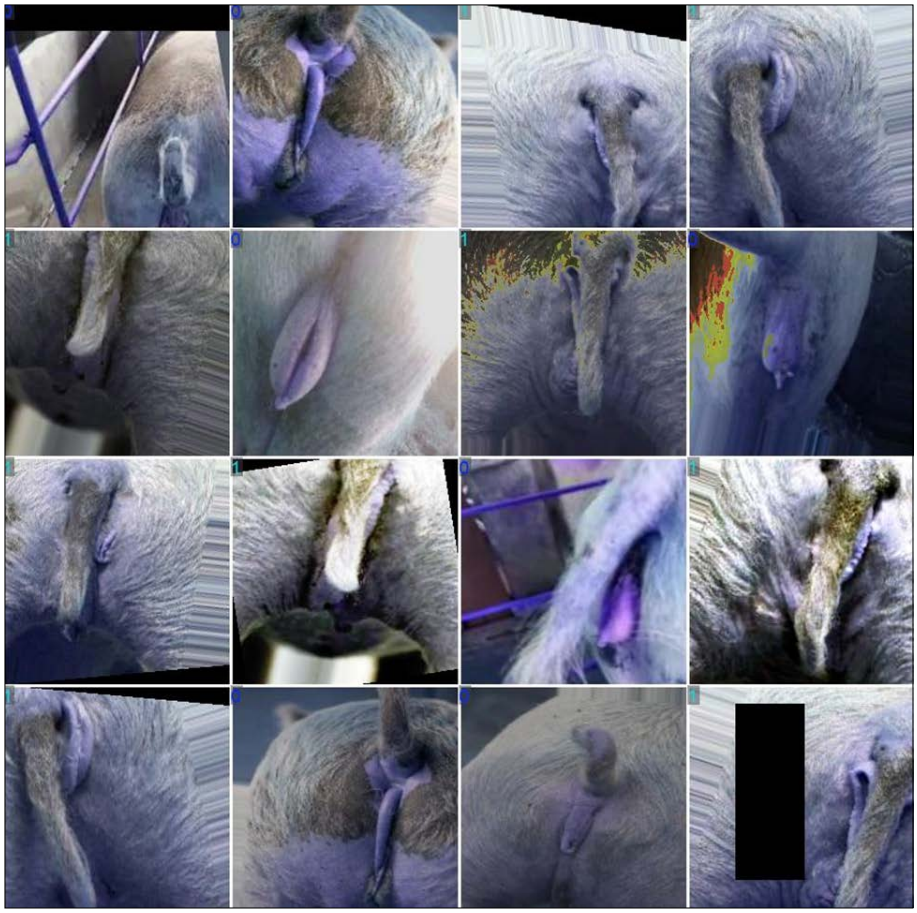

Fig 7: train batch2

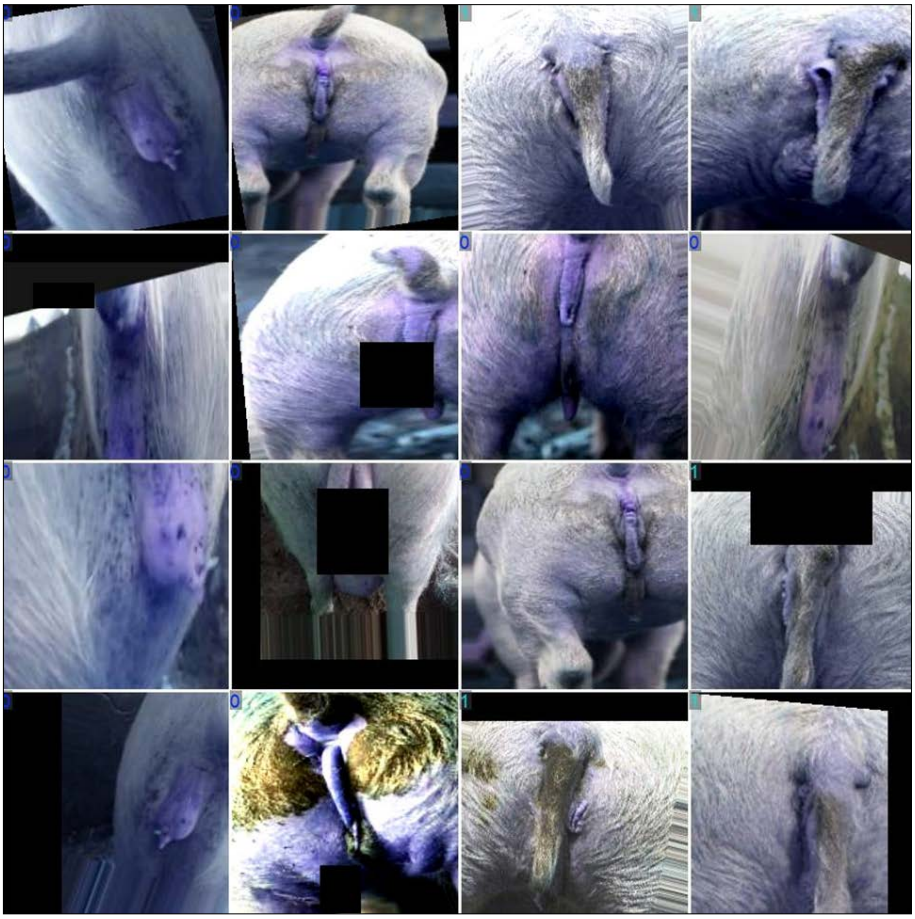

Fig 8: train batch440

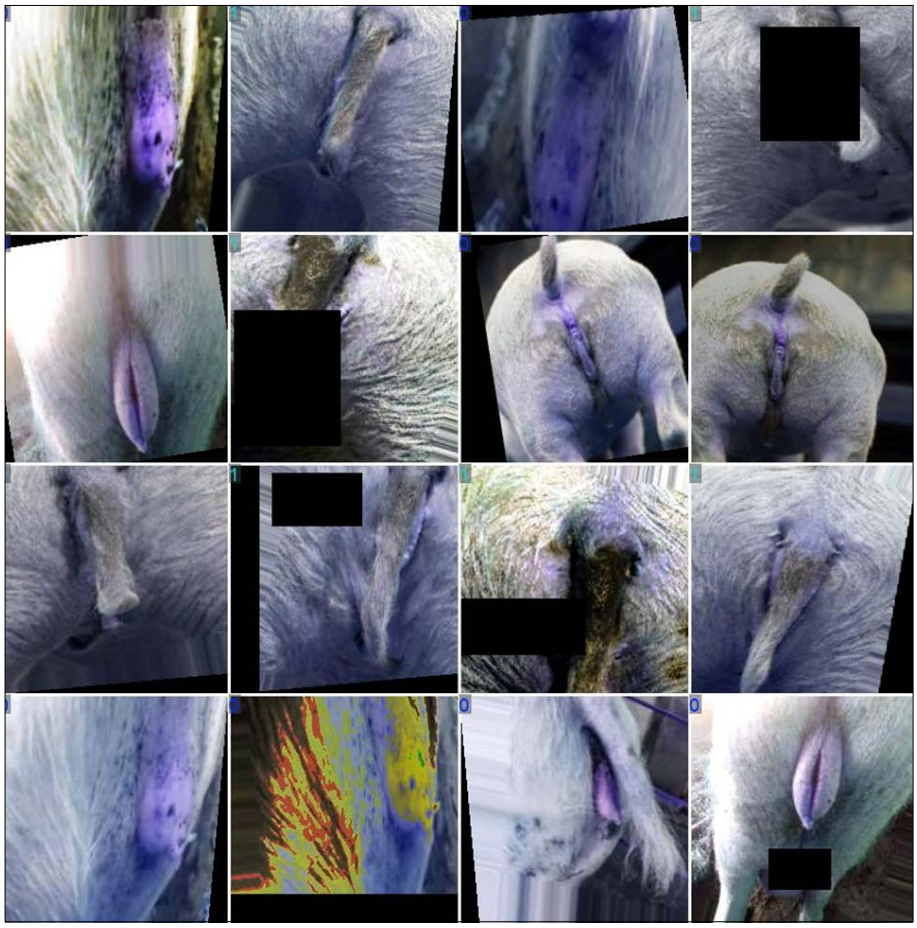

Fig 9: train batch441

Fig 10: train batch442

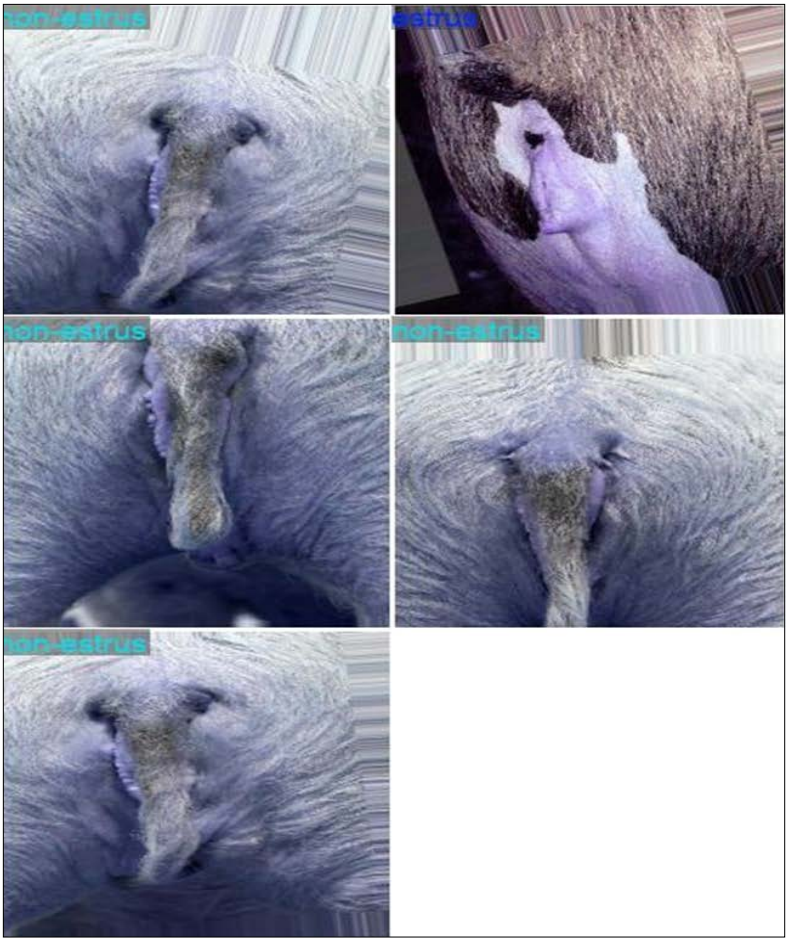

Fig 11: Value batch1 labels

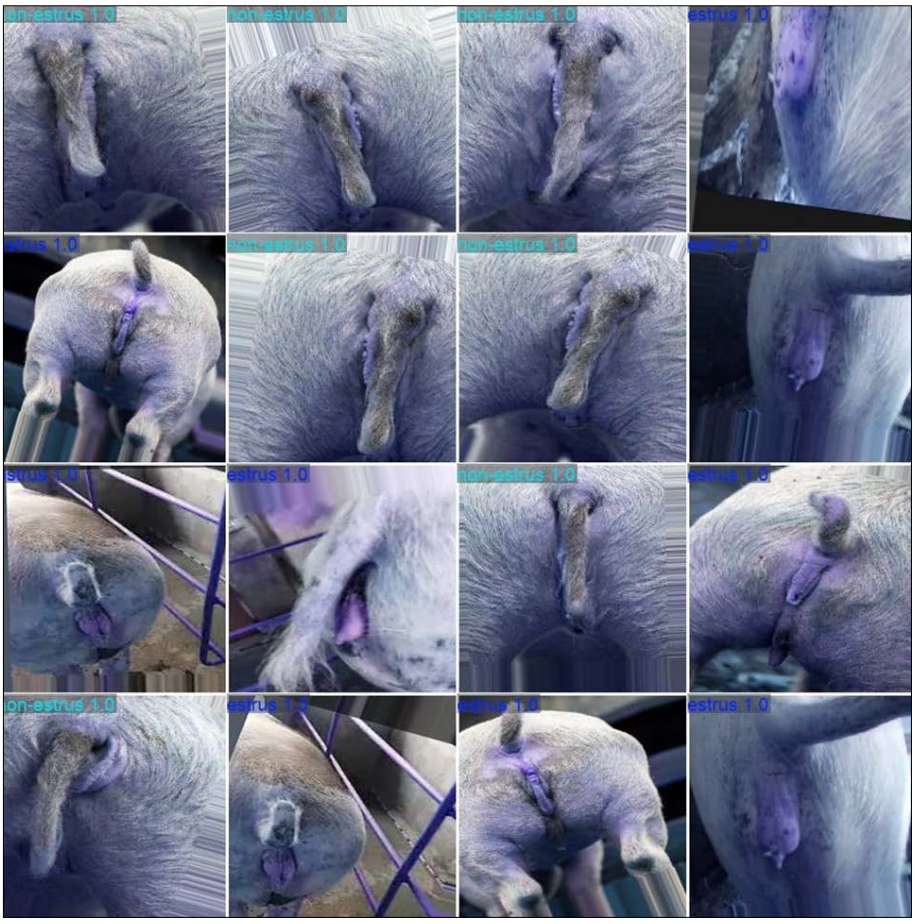

Fig 12: Value batch0 predicted

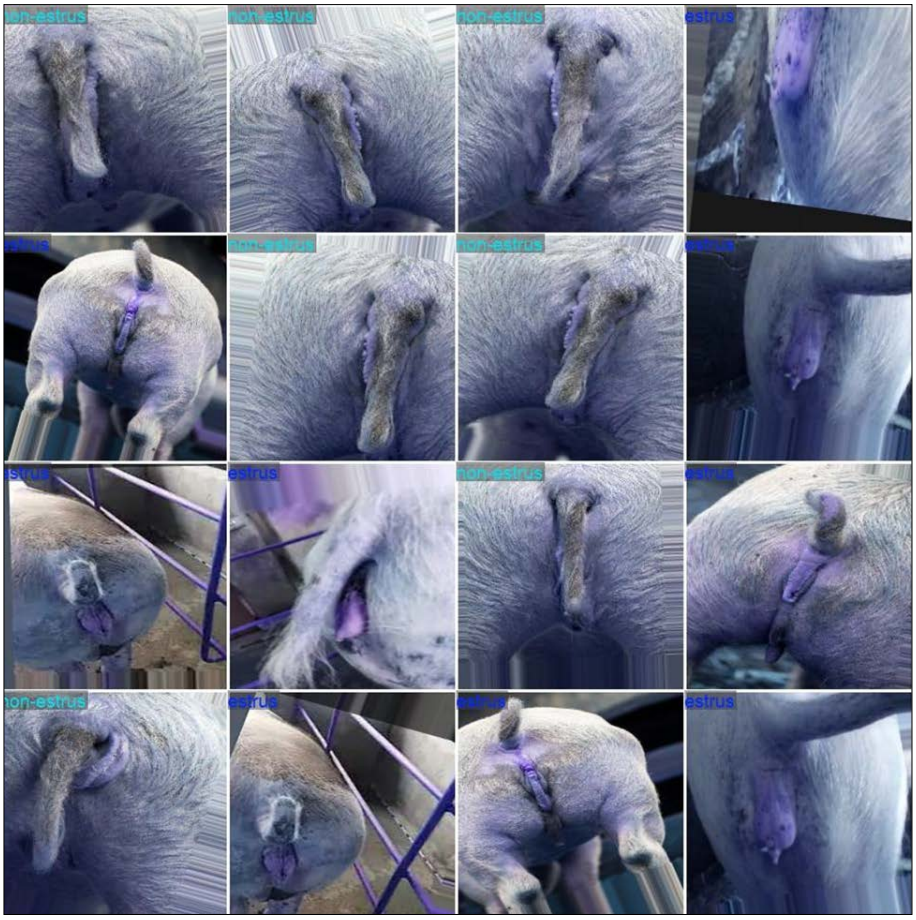

Fig 13: Value batch0 labels

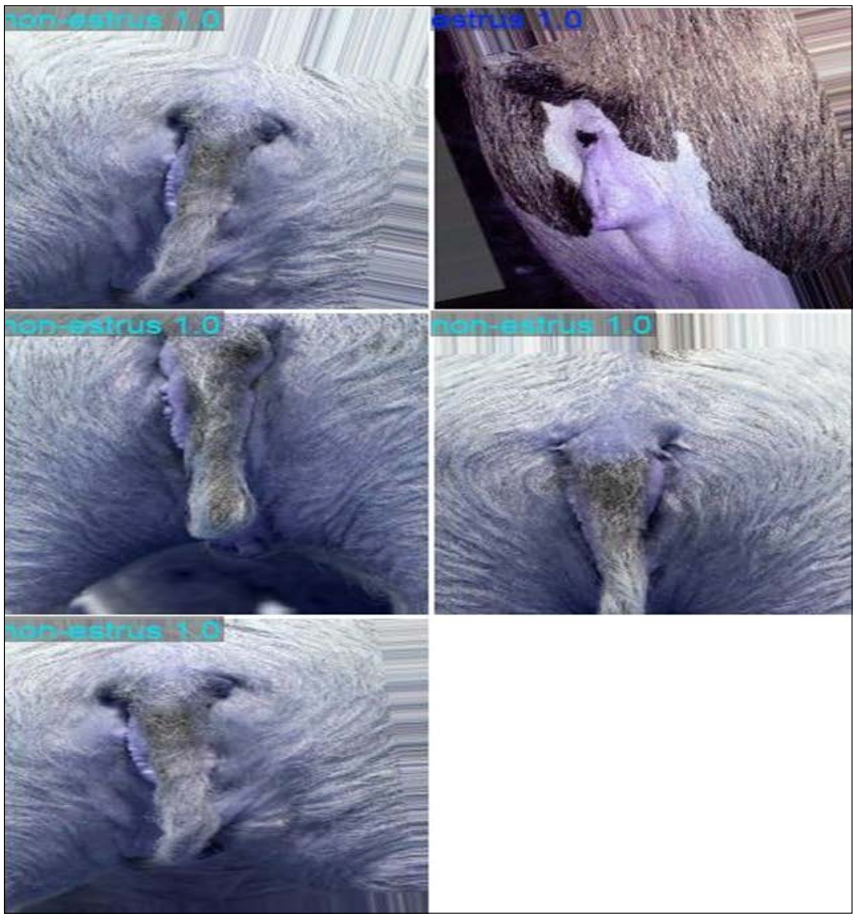

Fig 14: Value batch1 predicted

2. Confusion matrix and classification report

This session discusses Confusion Matrix and Classification report:

Confusion Matrix

The confusion matrix is a valuable tool for evaluating the performance of the model by showing the number of correct and incorrect predictions made for each class. Figure 4.12 shows the confusion matrix while figure 4.13 shows the normalized confusion matrix

Terminology Used

Term	Meaning
TP (True Positive)	Estrus Sow correctly classified as estrus
TN (True Negative)	Non-estrus Sow correctly classified as non-estrus
FP (False Positive)	Estrus Sow incorrectly classified as non-estrus
FN (False Negative)	Non-estrus Sow incorrectly classified as estrus

Calculation for Confusion Matrix

For each class:

- Precision = TP / (TP + FP)
- Recall = TP / (TP + FN)
- F1-Score = 2 × (Precision × Recall) / (Precision + Recall)

Where:

- TP = True Positives
- FP = False Positives
- FN = False Negatives

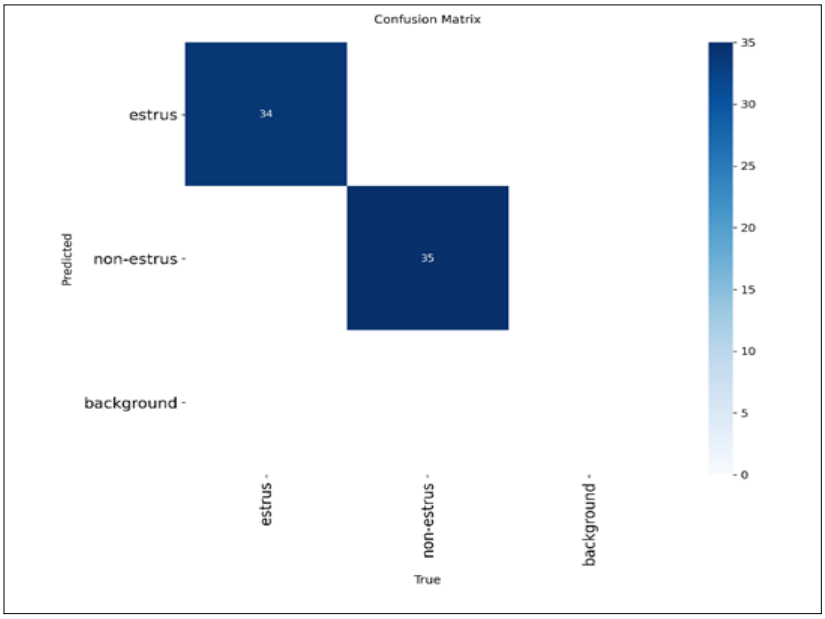

Fig 15: Confusion matrix heatmap

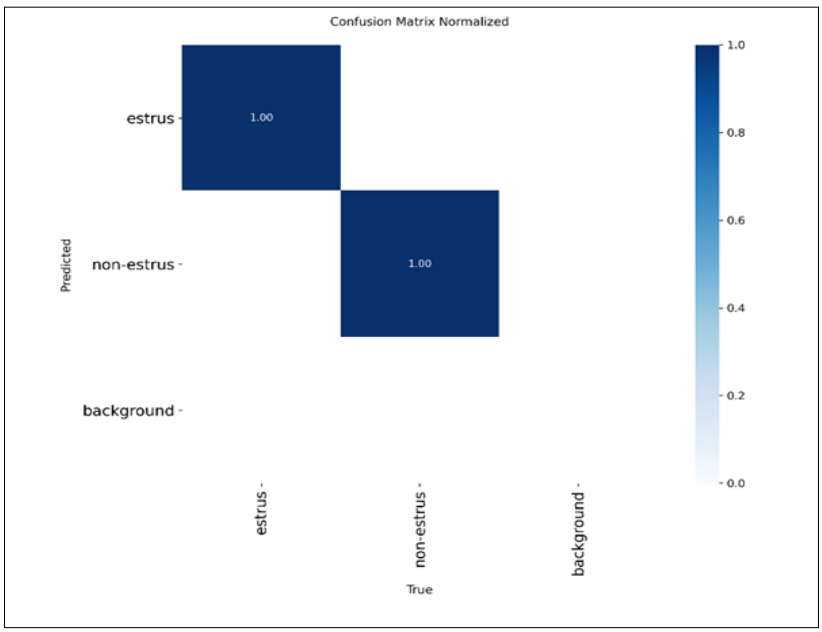

Fig 16: normalized confusion matrix heatmap

From the confusion matrix the following values are gotten
TP = 35
FP = 0
FN = 2
TN = 34
Hence the performance metrics values are as follows
Accuracy = 0.9718
Precision = 1.000
Recall = 0.9459
F1-Score = 0.9722
Specificity = 1.000

3. Performance Evaluation

Estrus detective System performance

Table 3: Outputs of the estrus detective system

	Metric	Value
0	Accuracy	0.97
1	Precision	1.00
2	Recall	0.95
3	F1-Score	0.97
4	Specificity	1.00

The developed system was compared to the existing system by Cristina *et al*. (2025) [6] which utilized the random forest model for detection of estrus in Sows table 4.3 ANF figure 4.15 shows the comparison

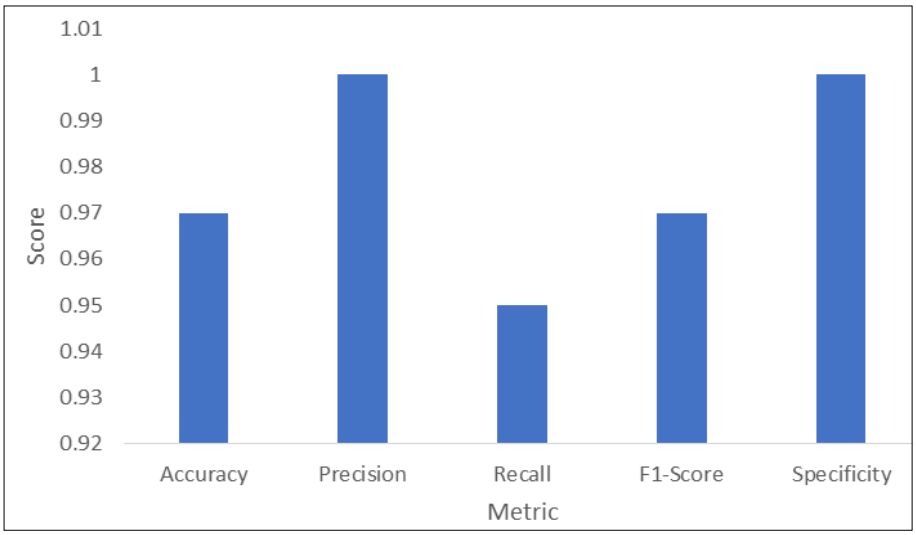

Fig 17: Performance of the developed model

Table 4: Comparison of the developed model with existing system

Metric	Existing System (Random Forest)	Developed System
Accuracy	87%	97%
Precision	90%	100%
Recall	85%	95%
F1-Score	87%	97%
Specificity	90%	100%

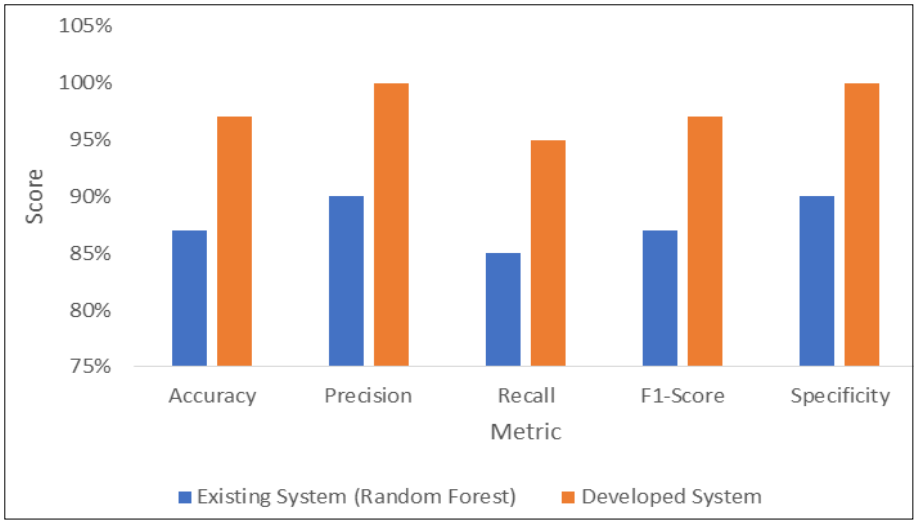

Fig 18: Performance comparison chart between the existing system and the developed system

The developed model consistently outperforms the traditional random forest based model across all key metrics. The biggest gains are seen in precision aand specificity, indicating better precision

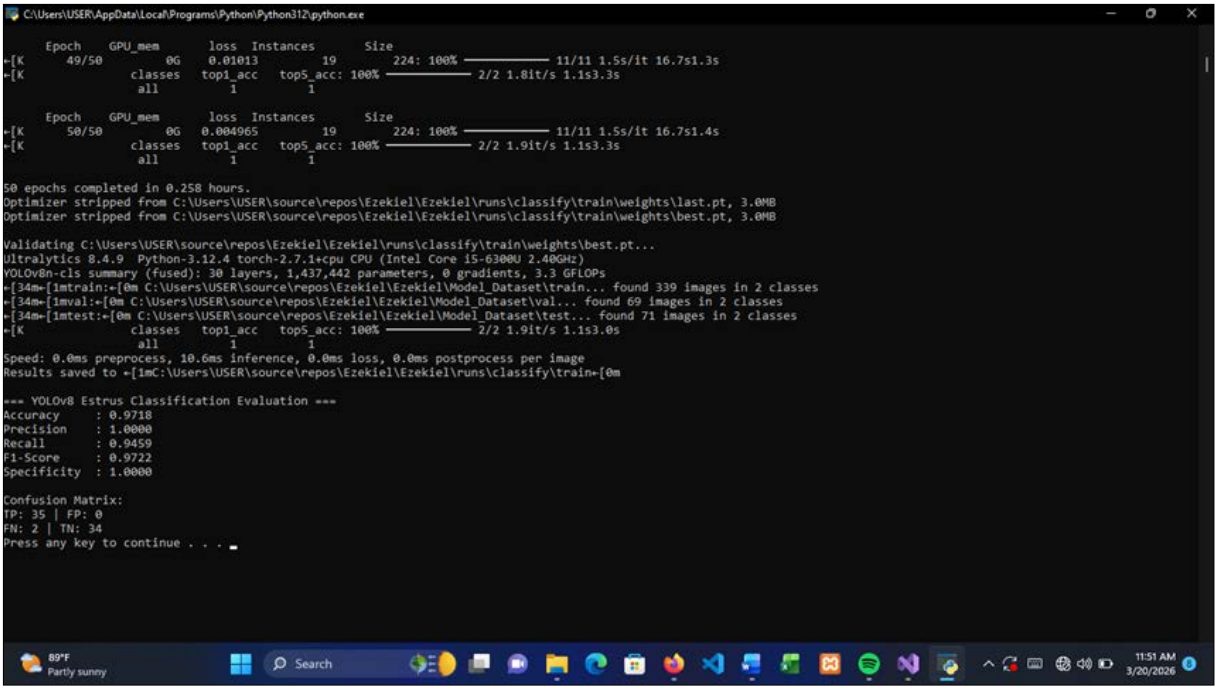

Fig 19: Model training page

Conclusion

The study has evaluated a deep-learning based estrus detection system and demonstrated its reliability and effectiveness as a modern tool for accurately predicting various retinal diseases. By leveraging the YOLOv8 model, the system has shown a remarkable ability to classify estrus and non-estrus sows with a high level of accuracy. This advancement plays a critical role in supporting early detection, which is essential in swine reproductive management. During testing and validation phases, the model achieved strong performance metrics such as high accuracy, precision, recall, and F1-scores, all of which affirm the robustness and reliability of the system. Additionally, the system's lightweight design and scalable architecture make it suitable for deployment in diverse environments, including rural or under-resourced healthcare settings. It provides healthcare professionals with a decision-support tool that not only improves diagnostic speed but also contributes to better patient management and outcomes. Ultimately, this system bridges the gap between modern AI technology and practical agricultural application, promoting swine reproductive management.

References

1. Egheneji AW, Edje AE, Obidike CA. Multi-objective cooperative particle swarm optimization resource scheming technique in vehicular cloud infrastructure as a service platform. International Journal of Science and Research Archive,2026:18(03):755-763. Article DOI: https://doi.org/10.30574/ijsra.2026.18.3.0500
2. Almadani I, Abuhussein M, Robinson AL. YOLOv8-Based Estimation of Estrus in Sows Through Reproductive Organ Swelling Analysis Using a Single Camera, 2024, 898–913.
3. Almadani I, Ramos B, Abuhussein M, Robinson AL. Advanced Swine Management: Infrared Imaging for Precise Localization of Reproductive Organs in Livestock Monitoring, 2024, 446–460.
4. Cai J, Liu W, Liu T, Wang F, Li Z, Wang X, et al. APO-CViT : A Non-Destructive Estrus Detection Method for Breeding Pigs Based on Multimodal Feature Fusion, 2025.
5. Chen P, Yin D, Yang B, Tang W. A Fusion Feature for the Oestrous Sow Sound Identification Based on Convolutional Neural Networks A Fusion Feature for the Oestrous Sow Sound Identification Based on Convolutional Neural Networks, n.d., 1–6. https://doi.org/10.1088/1742-6596/2203/1/012049
6. Cristina L, Moura S, Mendes JP, Ferreira YM, Sousa R, Amaral V, et al. Combined Infrared Thermography and Agitated Behavior in Sows Improve Estrus Detection When Applied to Supervised Machine Learning Algorithms, 2025, 1–12.
7. Duan Y, Yang Y, Cao Y, Liu J, Li L, Cao R. Smart Agricultural Technology a multimodal deep learning network for precise detection of estrus and pseudo-estrus in sows ☆. Smart Agricultural Technology,2025:12:101279. https://doi.org/10.1016/j.atech.2025.101279
8. Obidike CA, Edje EA, Fasanmi EA. Multi schemes for dynamic task scheduling in cloud computinginfrastructure. Scientia Africana,2025:24(2 SE-Articles):79–88. https://doi.org/10.4314/sa.v24i2.
9. Sohan M, Sairam T, Author C. A Review on YOLOv8 and its Advancements, n.d.
10. Xue H, Chen J, Ding Q, Sun Y, Shen M, Liu L, et al. Automatic detection of sow posture and estrus based on convolutional neural network, 2022, (October), 1–13. https://doi.org/10.3389/fphy.2022.1037129
11. Zhao M, Duan Y, Gao T, Gao X, Hu G, Cao R, et al. A Lightweight Model for Small-Target Pig Eye Detection in Automated Estrus Recognition, 2025, 1.
12. Zheng H, Zhang H, Song S, Wang Y, Liu T. Automatic detection of sow estrus using a lightweight real-time detector and thermal images,2023:16(3):194–207. https://doi.org/10.25165/j.ijabe.20231603.7711